A Voltage-Controlled PFC Cuk Converter-Based PMBLDCM Drive for Air-Conditioners

Sanjeev Singh, *Member, IEEE*, and Bhim Singh, *Fellow, IEEE*

***Abstract*—This paper deals with a Cuk dc–dc converter as a single-stage power-factor-correction converter for a permanent-magnet (PM) brushless dc motor (PMBLDCM) fed through a diode bridge rectifier from a single-phase ac mains. A three-phase voltage-source inverter is used as an electronic commutator to operate the PMBLDCM driving an air-conditioner compressor. The speed of the compressor is controlled to achieve optimum air-conditioning using a concept of the voltage control at dc link proportional to the desired speed of the PMBLDCM. The stator currents of the PMBLDCM during step change in the reference speed are controlled within the specified limits by an addition of a rate limiter in the reference dc link voltage. The proposed PMBLDCM drive (PMBLDCMD) is designed and modeled, and its performance is evaluated in Matlab–Simulink environment. Simulated results are presented to demonstrate an improved power quality at ac mains of the PMBLDCMD system in a wide range of speed and input ac voltage. Test results of a developed controller are also presented to validate the design and model of the drive.**

***Index Terms*—Air-conditioner, Cuk converter, power factor (PF) correction (PFC), permanent-magnet (PM) brushless dc motor (PMBLDCM), voltage control, voltage-source inverter (VSI).**

I. Introduction

THE use of a permanent-magnet (PM) brushless dc motor (PMBLDCM) in low-power appliances is increasing because of its features of high efficiency, wide speed range, and low maintenance [1]–[4]. It is a rugged three-phase synchronous motor due to the use of PMs on the rotor. The commutation in a PMBLDCM is accomplished by solid state switches of a three-phase voltage-source inverter (VSI). Its application to the compressor of an air-conditioning (Air-Con) system results in an improved efficiency of the system if operated under speed control while maintaining the temperature in the air-conditioned zone at the set reference consistently. The Air-Con exerts constant torque (i.e., rated torque) on the PMBLDCM while operated in speed control mode. The Air-Con system with PMBLDCM has low running cost, long life, and reduced mechanical and electrical stresses compared to a single-phase induction motor-based Air-Con system operating in "on/off" control mode.

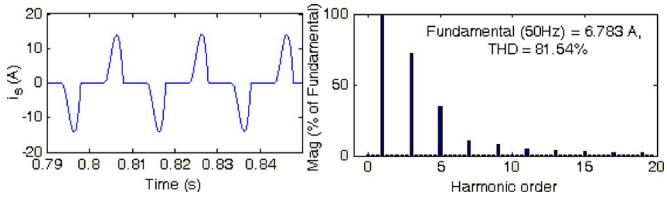

Fig. 1. Current waveform at ac mains and its harmonic spectra for the PMBLDCM drive (PMBLDCMD) without PFC.

A PMBLDCM has the developed torque proportional to its phase current and its back electromotive force (EMF), which is proportional to the speed [1]–[4]. Therefore, a constant current in its stator windings with variable voltage across its terminals maintains constant torque in a PMBLDCM under variable speed operation. A speed control scheme is proposed which uses a reference voltage at dc link proportional to the desired speed of the permanent-magnet brushless direct current (PMBLDC) motor. However, the control of VSI is only used for electronic commutation based on the rotor position signals of the PMBLDC motor.

The PMBLDCMD is fed from a single-phase ac supply through a diode bridge rectifier (DBR) followed by a capacitor at dc link. It draws a pulsed current as shown in Fig. 1, with a peak higher than the amplitude of the fundamental input current at ac mains due to an uncontrolled charging of the dc link capacitor. This results in poor power quality (PQ) at ac mains in terms of poor power factor (PF) of the order of 0.728, high total harmonic distortion (THD) of ac mains current at the value of 81.54%, and high crest factor (CF) of the order of 2.28. Therefore, a PF correction (PFC) converter among various available converter topologies [5], [6] is almost inevitable for a PMBLDCMD. Moreover, the PQ standards for low power equipments, such as IEC 61000-3-2 [7], emphasize on low harmonic contents and near unity PF current to be drawn from ac mains by these drives.

There are very few publications regarding PFC in PMBLDCMDs despite many PFC topologies for switched-mode power supply and battery charging applications. This paper deals with an application of a PFC converter for the speed control of a PMBLDCMD. For the proposed voltage-controlled drive, a Cuk dc–dc converter is used as a PFC converter because of its continuous input and output currents, small output filter, and wide output voltage range as compared to other single switch converters [8]–[10]. Moreover, apart from PQ improvement at ac mains, it controls the voltage at dc link for the desired speed of the Air-Con. The detailed

Manuscript received October 16, 2010; revised June 11, 2011 and October 19, 2011; accepted December 12, 2011. Date of publication January 2, 2012; date of current version March 21, 2012. Paper 2010-IACC-410.R2, presented at the 2010 Industry Applications Society Annual Meeting, Houston, TX, October 3–7, and approved for publication in the IEEE TRANSACTIONS ON INDUSTRY APPLICATIONS by the Industrial Automation and Control Committee of the IEEE Industry Applications Society.

S. Singh is with the Department of Electrical and Instrumentation Engineering, Sant Longowal Institute of Engineering and Technology, Longowal 148106, India (e-mail: sschauhan.sdl@gmail.com).

B. Singh is with the Department of Electrical Engineering, Indian Institute of Technology Delhi, New Delhi 110016, India (e-mail: bhimsinghiitd@gmail.com).

Digital Object Identifier 10.1109/TIA.2011.2182329

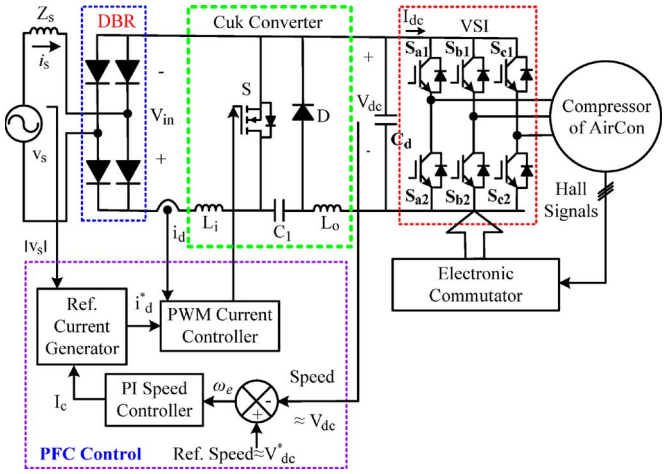

Fig. 2. Control scheme of the proposed Cuk PFC converter-fed VSI-based PMBLDCMD.

modeling, design, and performance evaluation of the proposed drive are presented for an air-conditioner driven by a 0.816-kW 1500-r/min PMBLDC motor.

II. Proposed Speed Control Scheme of PMBLDC Motor for Air-Conditioner

Fig. 2 shows the proposed speed control scheme which is based on the control of the dc link voltage reference as an equivalent to the reference speed. However, the rotor position signals acquired by Hall-effect sensors are used by an electronic commutator to generate switching sequence for the VSI feeding the PMBLDC motor, and therefore, rotor position is required only at the commutation points [1]–[4].

The Cuk dc–dc converter controls the dc link voltage using capacitive energy transfer which results in nonpulsating input and output currents [8]. The proposed PFC converter is operated at a high switching frequency for fast and effective control with additional advantage of a small size filter. For high-frequency operation, a metal–oxide–semiconductor field-effect transistor (MOSFET) is used in the proposed PFC converter, whereas insulated gate bipolar transistors (IGBTs) are used in the VSI bridge feeding the PMBLDCM because of its operation at lower frequency compared to the PFC converter.

The PFC control scheme uses a current multiplier approach with a current control loop inside the speed control loop for continuous-conduction-mode operation of the converter. The control loop begins with the processing of voltage error (V_e), obtained after the comparison of sensed dc link voltage $(V_{\rm dc})$ and a voltage $(V^*_{\rm dc})$ equivalent to the reference speed, through a proportional–integral (PI) controller to give the modulating control signal (I_c). This signal (I_c) is multiplied with a unit template of input ac voltage to get the reference dc current (I^*_d) and compared with the dc current (I_d) sensed after the DBR. The resultant current error (I_e) is amplified and compared with a sawtooth carrier wave of fixed frequency (f_s) to generate the pulsewidth modulation (PWM) pulse for the Cuk converter. Its duty ratio (D) at a switching frequency (f_s) controls the dc link voltage at the desired value. For the control of current to PMBLDCM through VSI during the step change of the reference voltage due to the change in the reference speed, a rate limiter is introduced, which limits the stator current of the PMBLDCM within the specified value which is considered as double the rated current in this work.

III. Design of PFC Cuk Converter-Based PMBLDCMD

The proposed PFC Cuk converter is designed for a PMBLDCMD with main considerations on the speed control of the AirCon and PQ improvement at ac mains. The dc link voltage of the PFC converter is given as

$$V_{\rm dc} = V_{\rm in} D/(1-D) \tag{1}$$

where $V_{\rm in}$ is the average output of the DBR for a given ac input voltage (V_s) related as

$$V_{\rm in} = 2\sqrt{2}V_s/\pi. \tag{2}$$

The Cuk converter uses a boost inductor (L_i) and a capacitor (C_1) for energy transfer. Their values are given as

$$L_i = DV_{\rm in}/\{f_s(\Delta I_{\rm Li})\} \tag{3}$$
$$C_1 = DI_{\rm dc}/\{f_s \Delta V_{\rm C1}\} \tag{4}$$

where $\Delta I_{\rm Li}$ is a specified inductor current ripple, $\Delta V_{\rm C1}$ is a specified voltage ripple in the intermediate capacitor (C_1), and $I_{\rm dc}$ is the current drawn by the PMBLDCM from the dc link.

A ripple filter is designed for ripple-free voltage at the dc link of the Cuk converter. The inductance (L_o) of the ripple filter restricts the inductor peak-to-peak ripple current $(\Delta I_{\rm Lo})$ within a specified value for the given switching frequency (f_s), whereas the capacitance (C_d) is calculated for the allowed ripple in the dc link voltage $(\Delta V_{\rm Cd})$ [7], [8]. The values of the ripple filter inductor and capacitor are given as

$$L_o = (1-D)V_{\rm dc}/\{f_s(\Delta I_{\rm Lo})\} \tag{5}$$
$$C_d = I_{\rm dc}/(2\omega \Delta V_{\rm Cd}). \tag{6}$$

The PFC converter is designed for a base dc link voltage of $V_{\rm dc} = 298$ V at $V_s = 220$ V for $f_s = 40$ kHz, $I_s = 4.5$ A, $\Delta I_{\rm Li} = 0.45$ A (10% of $I_{\rm dc}$), $I_{\rm dc} = 3.5$ A, $\Delta I_{\rm Lo} = 3.5$ A ($\approx I_{\rm dc}$), $\Delta V_{\rm Cd} = 4$ V (1% of V_o), and $\Delta V_{\rm C1} = 220$ V ($\approx V_s$). The design values are obtained as $L_i = 6.61$ mH, $C_1 = 0.3$ μF, $L_o = 0.82$ mH, and $C_d = 1590$ μF.

IV. Modeling of PFC Converter-Based PMBLDCMD

The PFC converter and PMBLDCMD are the main components of the proposed drive, which are modeled by mathematical equations, and a combination of these models represents the complete model of the drive.

A. PFC Converter

The modeling of the PFC converter consists of the modeling of a speed controller, a reference current generator, and a PWM controller as given hereinafter.

1) Speed Controller: The speed controller is a PI controller which tracks the reference speed as an equivalent reference voltage. If, at the kth instant of time, $V^*_{\rm dc}(k)$ is the reference

TABLE I
ELECTRONIC COMMUTATOR OUTPUT BASED ON THE HALL-EFFECT SENSOR SIGNALS [6], [11]

Hall Signals			*Switching Signals*					
H_a	H_b	H_c	S_{a1}	S_{a2}	S_{b1}	S_{b2}	S_{c1}	S_{c2}
0	0	0	0	0	0	0	0	0
0	0	1	0	0	0	1	1	0
0	1	0	0	1	1	0	0	0
0	1	1	0	1	0	0	1	0
1	0	0	1	0	0	0	0	1
1	0	1	1	0	0	1	0	0
1	1	0	0	0	1	0	0	1
1	1	1	0	0	0	0	0	0

dc link voltage and $V_{\rm dc}(k)$ is the voltage sensed at the dc link, then the voltage error $V_e(k)$ is given as

$$V_e(k) = V^*_{\rm dc}(k) - V_{\rm dc}(k). \tag{7}$$

The PI controller output $I_c(k)$ at the kth instant after processing the voltage error $V_e(k)$ is given as

$$I_c(k) = I_c(k-1) + K_p\{V_e(k) - V_e(k-1)\} + K_i V_e(k) \tag{8}$$

where K_p and K_i are the proportional and integral gains of the PI controller.

2) Reference Current Generator: The reference current at the input of the Cuk converter (i^*_d) is

$$i^*_d = I_c(k) u_{\rm Vs} \tag{9}$$

where $u_{\rm Vs}$ is the unit template of the ac mains voltage, calculated as

$$u_{\rm Vs} = v_d/V_{\rm sm}; \quad v_d = |v_s|; \quad v_s = V_{\rm sm}\sin\omega t \tag{10}$$

where $V_{\rm sm}$ and ω are the amplitude (in volts) and frequency (in radians per second) of the ac mains voltage.

3) PWM Controller: The reference input current of the Cuk converter (i^*_d) is compared with its current (i_d) sensed after DBR to generate the current error $\Delta i_d = (i^*_d - i_d)$. This current error is amplified by gain k_d and compared with fixed frequency (f_s) sawtooth carrier waveform $m_d(t)$ [6] to get the switching signal for the MOSFET of the PFC Cuk converter as

$$\text{if} \quad k_d \Delta i_d > m_d(t) \quad \text{then } S = 1 \text{ else } S = 0 \tag{11}$$

where S denotes the switching of the MOSFET of the Cuk converter as shown in Fig. 2 and its values "1" and "0" represent "on" and "off" conditions, respectively.

B. PMBLDCMD

The PMBLDCMD consists of an electronic commutator, a VSI, and a PMBLDCM.

1) Electronic Commutator: The electronic commutator uses signals from Hall-effect position sensors to generate the switching sequence for the VSI as shown in Table I [6], [11].

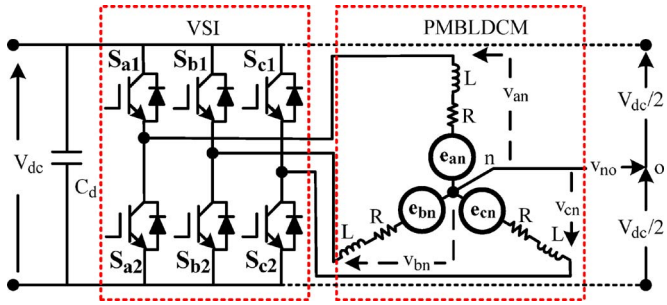

Fig. 3. Equivalent circuit of a VSI-fed PMBLDCMD.

2) VSI: The output of VSI to be fed to phase "a" of the PMBLDC motor is calculated from the equivalent circuit of a VSI-fed PMBLDCM shown in Fig. 3 as

$$v_{\rm ao} = (V_{\rm dc}/2) \quad \text{for } S_{\rm a1} = 1 \tag{12}$$
$$v_{\rm ao} = (-V_{\rm dc}/2) \quad \text{for } S_{\rm a2} = 1 \tag{13}$$
$$v_{\rm ao} = 0 \quad \text{for } S_{\rm a1} = 0, \text{ and } S_{\rm a2} = 0 \tag{14}$$
$$v_{\rm an} = v_{\rm ao} - v_{\rm no} \tag{15}$$

where $v_{\rm ao}$, $v_{\rm bo}$, $v_{\rm co}$, and $v_{\rm no}$ are the voltages the three phases (a, b, and c) and neutral point (n) with respect to the virtual midpoint of the dc link voltage shown as "o" in Fig. 3. The voltages $v_{\rm an}$, $v_{\rm bn}$, and $v_{\rm cn}$ are the voltages of the three phases with respect to the neutral terminal of the motor (n), and $V_{\rm dc}$ is the dc link voltage. The values 1 and 0 for $S_{\rm a1}$ or $S_{\rm a2}$ represent the "on" and "off" conditions of respective IGBTs of the VSI.

The voltages for the other two phases of the VSI feeding the PMBLDC motor, i.e., $v_{\rm bo}$, $v_{\rm co}$, $v_{\rm bn}$, and $v_{\rm cn}$, and the switching pattern of the other IGBTs of the VSI (i.e., $S_{\rm b1}$, $S_{\rm b2}$, $S_{\rm c1}$, and $S_{\rm c2}$) are generated in a similar way.

3) PMBLDC Motor: The PMBLDCM is modeled in the form of a set of differential equations [11] given as

$$v_{\rm an} = {\rm R}i_{\rm a} + p\lambda_{\rm a} + e_{\rm an} \tag{16}$$
$$v_{\rm bn} = {\rm R}i_{\rm b} + p\lambda_{\rm b} + e_{\rm bn} \tag{17}$$
$$v_{\rm cn} = {\rm R}i_{\rm c} + p\lambda_{\rm c} + e_{\rm cn}. \tag{18}$$

In these equations, p represents the differential operator (d/dt), $i_{\rm a}$, $i_{\rm b}$, and $i_{\rm c}$ are currents, $\lambda_{\rm a}$, $\lambda_{\rm b}$, and $\lambda_{\rm c}$ are flux linkages, and $e_{\rm an}$, $e_{\rm bn}$, and $e_{\rm cn}$ are phase-to-neutral back EMFs of PMBLDCM, in respective phases; R is the resistance of motor windings/phase.

Moreover, the flux linkages can be represented as

$$\lambda_{\rm a} = L_s i_{\rm a} - M(i_{\rm b} + i_{\rm c}) \tag{19}$$
$$\lambda_{\rm b} = L_s i_{\rm b} - M(i_{\rm a} + i_{\rm c}) \tag{20}$$
$$\lambda_{\rm c} = L_s i_{\rm c} - M(i_{\rm b} + i_{\rm a}) \tag{21}$$

where L_s is the self-inductance/phase and M is the mutual inductance of PMBLDCM winding/phase.

The developed torque T_e in the PMBLDCM is given as

$$T_e = (e_{\rm an}i_{\rm a} + e_{\rm bn}i_{\rm b} + e_{\rm cn}i_{\rm c})/\omega_r \tag{22}$$

where ω_r is the motor speed in radians per second.

Since PMBLDCM has no neutral connection

$$i_{\rm a} + i_{\rm b} + i_{\rm c} = 0. \tag{23}$$

From (15)–(21) and (23), the voltage $(v_{\rm no})$ between the neutral point (n) and midpoint of the dc link (o) is given as

$$v_{\rm no} = \{v_{\rm ao} + v_{\rm bo} + v_{\rm co} - (e_{\rm an} + e_{\rm bn} + e_{\rm cn})\}/3. \tag{24}$$

From (19)–(21) and (23), the flux linkages are given as

$$\lambda_{\rm a} = (L_s + M)i_{\rm a}, \quad \lambda_{\rm b} = (L_s + M)i_{\rm b}, \quad \lambda_{\rm c} = (L_s + M)i_{\rm c}. \tag{25}$$

From (16)–(18) and (25), the current derivatives in generalized state-space form are given as

$$\mathrm{pi}_x = (v_{\rm xn} - i_x R - e_{\rm xn})/(L_s + M) \tag{26}$$

where x represents phase a, b, or c.

The back EMF is a function of rotor position (θ) as

$$e_{\rm xn} = K_b f_x(\theta)\omega_r \tag{27}$$

where x can be phase a, b, or c and accordingly $f_x(\theta)$ represents a function of rotor position with a maximum value ± 1, identical to trapezoidal induced EMF, given as

$$f_{\rm a}(\theta) = 1 \quad \text{for } 0 < \theta < 2\pi/3 \tag{28}$$
$$f_{\rm a}(\theta) = 1\{(6/\pi)(\pi - \theta)\} - 1 \quad \text{for } 2\pi/3 < \theta < \pi \tag{29}$$
$$f_{\rm a}(\theta) = -1 \quad \text{for } \pi < \theta < 5\pi/3 \tag{32}$$
$$f_{\rm a}(\theta) = \{(6/\pi)(\pi - \theta)\} + 1 \quad \text{for } 5\pi/3 < \theta < 2\pi. \tag{31}$$

The functions $f_{\rm b}(\theta)$ and $f_{\rm c}(\theta)$ are similar to $f_{\rm a}(\theta)$ with phase differences of 120° and 240°, respectively.

Therefore, the electromagnetic torque expressed as

$$T_e = K_b\{f_{\rm a}(\theta)i_{\rm a} + f_{\rm b} + f_{\rm c}(\theta)i_{\rm c}\}. \tag{32}$$

The mechanical equation of motion in speed derivative form is given as

$$p\omega_r = (P/2)(T_e - T_l - B\omega_r)/(J) \tag{33}$$

where ω_r is the derivative of rotor position θ, P is the number of poles, T_l is the load torque in newton meters, J is the moment of inertia in kilogram square meters, and B is the friction coefficient in newton meter seconds per radian.

The derivative of rotor position is given as

$$p\theta = \omega_r. \tag{34}$$

Equations (16)–(34) represent the dynamic model of the PMBLDC motor.

V. Performance Evaluation of PMBLDCMD

The proposed PMBLDCMD is modeled in Matlab–Simulink environment, and its performance is evaluated for an Air-Con compressor load. The compressor load is considered as a constant torque load equal to the rated torque (5.2 N · m) with variable speed as required by an Air-Con system. A 0.816-kW rating PMBLDCM is used to drive the air-conditioner, the speed of which is controlled effectively by controlling the dc link voltage. The detailed data of the motor are given in the Appendix. The performance of the proposed PFC drive is evaluated on the basis of various parameters such as THD and CF of the ac mains current and displacement power factor (DPF) and PF at different speeds of the motor as well as variable input ac voltage. For the performance evaluation of the proposed drive under input ac voltage variation, the dc link voltage is kept constant at 298 V which is equivalent to a 1500-r/min speed of the PMBLDCM. Figs. 4–8 and Tables II and III show the obtained results of the proposed PMBLDCMD in a wide range of the speed and the input ac voltage.

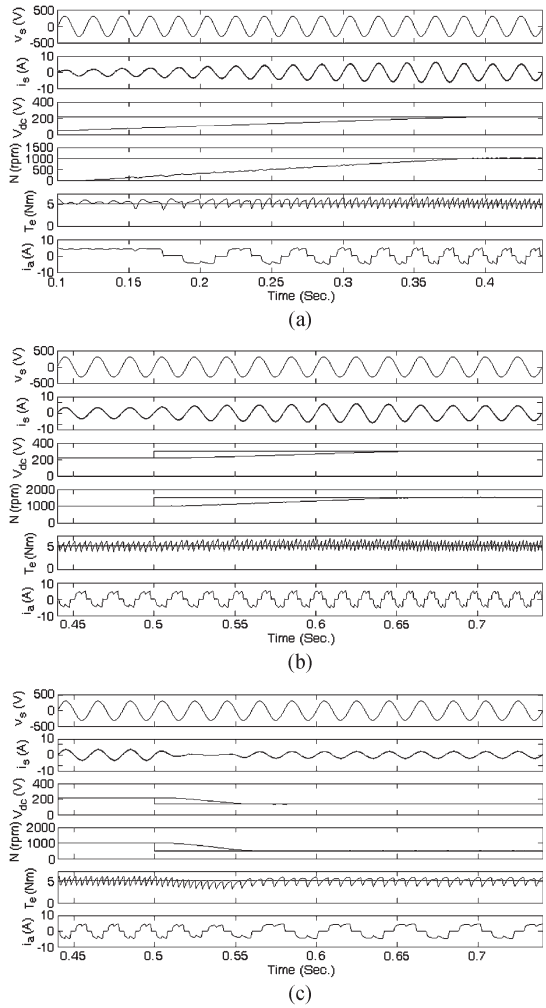

Fig. 4. Performance of the proposed PFC drive under speed control at 220-V ac input. (a) Starting performance of the proposed drive at 1000 r/min. (b) Proposed drive under speed control from 1000 to 1500 r/min. (c) Proposed drive under speed control from 1000 to 500 r/min.

A. Performance of PMBLDCMD During Starting

The performance of the PMBLDCMD during starting is evaluated while feeding it from 220-V ac mains with the reference speed set at 1000 r/min and rated torque. Fig. 4(a) shows the starting performance of the drive depicting voltage (v_s) and current (i_s) at ac mains, voltage at dc link $(V_{\rm dc})$, speed of motor (N), electromagnetic torque (T_e), and stator current of phase "a" $(i_{\rm a})$. A rate limiter is introduced in the reference voltage to limit the starting current of the motor as well as the charging current of the dc link capacitor. The PI

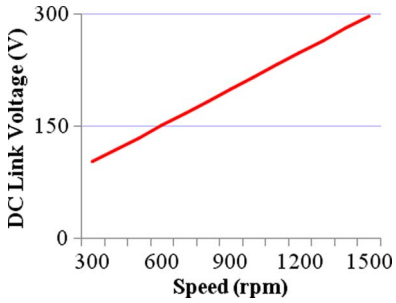

Fig. 5. Variation of dc link voltage with speed for proposed PFC drive at rated torque and 220-V ac input.

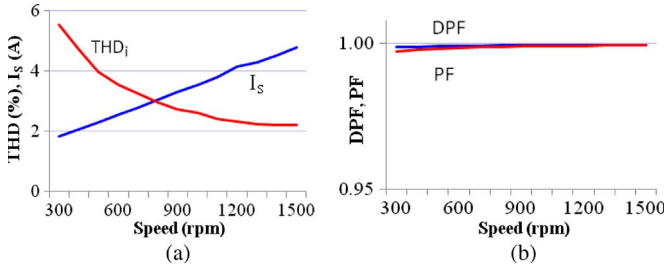

Fig. 6. PQ indices of proposed drive under speed control at rated torque and 220 V ac input. (a) Variation of I_s and its THD. (b) Variation of DPF and PF.

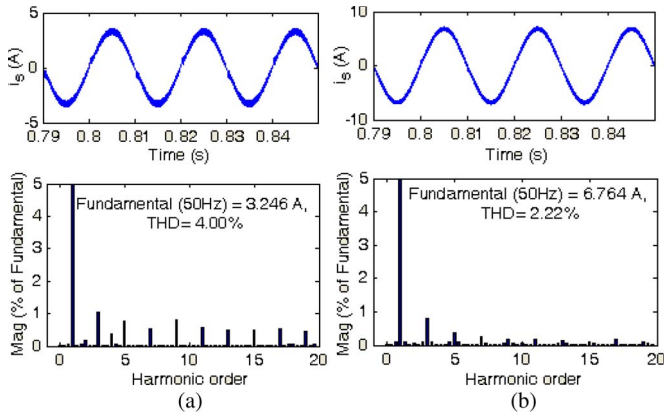

Fig. 7. Current waveform at input ac mains and its harmonic spectra for the proposed drive under steady-state condition at rated torque and 220 V ac input. (a) I_s and THD at 500 r/min. (b) I_s and THD at 1500 r/min.

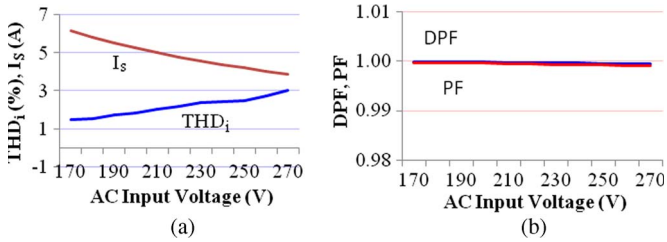

Fig. 8. PQ indices with input ac voltage variation at a constant dc link voltage of 298 V (≈1500 r/min). (a) Variation of I_s and its THD. (b)Variation of DPF and PF.

controller tracks the reference speed so that the motor attains reference speed smoothly within 0.375 s while keeping the stator current within the desired limits, i.e., double the rated value. The current waveform at input ac mains is in phase with the supply voltage demonstrating near unity PF during the starting.

TABLE II
PERFORMANCE OF THE PROPOSED DRIVE UNDER SPEED CONTROL AT 220-V INPUT AC VOLTAGE (V_s)

V_{DC} (V)	Speed (rpm)	THD_i (%)	DPF	PF	I_s (A)	Load (%)
104.0	300	5.55	0.9990	0.9975	1.82	20.0
119.0	400	4.74	0.9990	0.9979	2.05	26.7
135.5	500	4.00	0.9992	0.9984	2.30	33.3
151.5	600	3.55	0.9993	0.9987	2.55	40.0
167.5	700	3.25	0.9993	0.9988	2.79	46.7
183.5	800	2.97	0.9994	0.999	3.04	53.4
200.0	900	2.75	0.9995	0.9991	3.29	60.0
216.5	1000	2.63	0.9995	0.9992	3.54	66.7
233.0	1100	2.43	0.9996	0.9993	3.79	73.4
249.5	1200	2.33	0.9996	0.9993	4.15	80.0
265.5	1300	2.24	0.9997	0.9994	4.29	86.7
282.0	1400	2.23	0.9996	0.9994	4.53	93.4
298.0	1500	2.22	0.9996	0.9994	4.79	100.0

TABLE III
PQ INDICES WITH INPUT AC VOLTAGE (V_s) VARIATION AT 1500 r/min

V_{AC} (V)	THD_i (%)	DPF	PF	CF	I_s (A)
170	1.51	0.9998	0.9997	1.41	6.19
180	1.55	0.9998	0.9997	1.41	5.85
190	1.73	0.9997	0.9996	1.41	5.54
200	1.87	0.9998	0.9996	1.41	5.26
210	2.06	0.9997	0.9995	1.41	5.01
220	2.22	0.9996	0.9994	1.41	4.79
230	2.39	0.9996	0.9993	1.41	4.58
240	2.47	0.9996	0.9993	1.41	4.39
250	2.49	0.9995	0.9992	1.41	4.22
260	2.77	0.9995	0.9991	1.41	4.05
270	3.04	0.9995	0.999	1.41	3.90

B. *Performance of PMBLDCMD Under Speed Control*

Figs. 4–6 show the performance of PMBLDCMD for speed control at constant rated torque (5.2 N · m) and 220-V ac mains voltage during transient and steady-state conditions of the PMBLDCM.

1) Transient Condition: The performance of the drive during the speed transients is evaluated for acceleration and retardation of the compressor and shown in Fig. 4(b) and (c). The reference speed is changed from 1000 to 1500 r/min and from 1000 to 500 r/min for the performance evaluation of the compressor at rated load under speed control. It is observed that the speed control is fast and smooth in either directions, i.e., acceleration or retardation, with PF maintained at near unity value. Moreover, the stator current of PMBLDCM is less than

twice the rated current due to the rate limiter introduced in the reference voltage.

2) Steady-State Condition: The performance of PMBLDCMD under steady-state speed condition is obtained at different speeds as summarized in Table II which demonstrates the effectiveness of the proposed drive in a wide speed range. Fig. 5 shows the linear relation between motor speed and dc link voltage. Since the reference speed is decided by the reference voltage at dc link, it is observed that the control of the reference dc link voltage controls the speed of the motor.

C. PQ Performance of the PMBLDCMD

The performance of PMBLDCMD in terms of PQ indices, i.e., THD_i, CF, DPF, and PF, is obtained for different speeds as well as loads. These results are shown in Figs. 6 and 7 and Table II. Fig. 6(a) and (b) shows near unity PF and reduced THD of ac mains current in wide speed range of the PMBLDCM. The THD_i and harmonic spectra of ac mains current drawn by the proposed drive at 500- and 1500-r/min speeds are shown in Fig. 7(a) and (b) demonstrating less than 5% THD_i in a wide range of speed.

D. Performance of the PMBLDCMD Under Varying Input AC Voltage

The performance of the proposed PMBLDCMD is evaluated under varying input ac voltage at rated load (i.e., rated torque and rated speed) to demonstrate the effectiveness of the proposed drive for Air-Con system in various practical situations as summarized in Table III.

Fig. 8(a) and (b) shows the current and its THD at ac mains, DPF, and PF with ac input voltage. The THD of ac mains current is within specified limits of international norms [7] at near unity PF in a wide range of ac input voltage.

VI. Hardware Implementation

The designed proposed PFC controller is validated on a developed prototype of the drive in the laboratory. The developed hardware prototype for the speed control of PMBLDCMD uses a VSI along with a single-phase DBR and a dc capacitor. The data of a PMBLDC motor used for hardware implementation are given in the Appendix. The shaft of the PMBLDCM is coupled with a separately excited dc generator for application of mechanical load in terms of an equivalent electrical load.

For the implementation of the PWM current control algorithm, a digital signal processor (DSP) developed by Microchip named as dsPIC 30F6010 is used in this system, which also generates switching signals for VSI acting as an electronic commutator for the PMBLDCM. The switching signals for the VSI are obtained using the PWM channels of the dsPIC 30F6010, whereas the PWM signal for the PFC switch is generated at one of the I/O pins. The feedback signals of current and voltage are obtained using voltage and current sensor circuits designed in the voltage range of analog-to-digital converters of the processor. The unit template is generated using a zero-crossing detector circuit from the input ac mains voltage signal. The switching frequency of the PWM signal is kept constant at

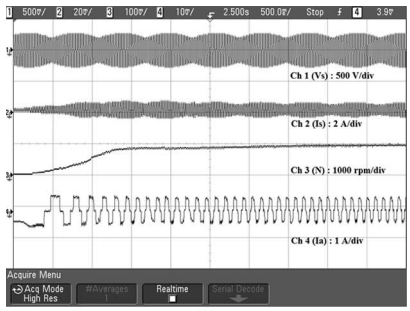

(a)

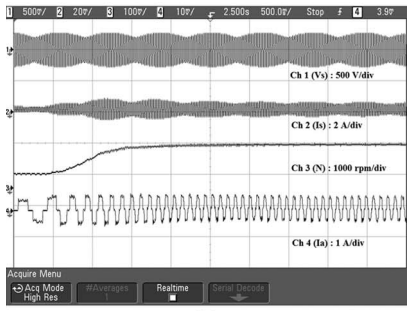

(b)

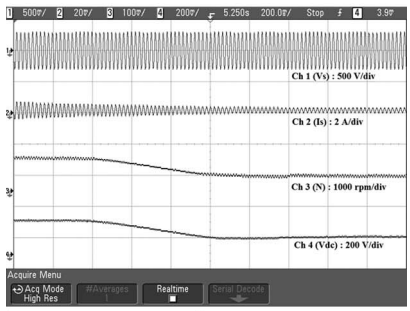

(c)

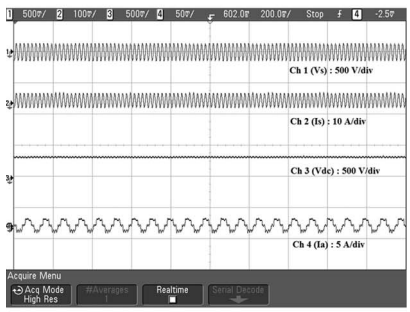

(d)

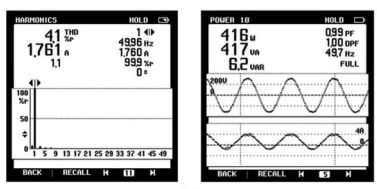

(e)

Fig. 9. (a) Test results of nonisolated Cuk PFC converter-fed PMBLDCMD during starting at reference speed of 1000 r/min. (b) Test results of nonisolated Cuk PFC converter-fed PMBLDCMD during speed control from 500 to 1500 r/min. (c) Test results of nonisolated Cuk PFC converter-fed PMBLDCMD demonstrating speed control through voltage control from 1000 to 500 r/min. (d) Test results of nonisolated Cuk PFC converter-fed PMBLDCMD during steady-state condition at reference speed of 1500 r/min. (e) Test results in terms of harmonic spectrum and waveform of ac mains current of nonisolated Cuk PFC converter-fed PMBLDCMD during steady-state condition at reference speed of 1500 r/min.

40 kHz, whereas it is the fundamental frequency corresponding to the speed of the motor for the electronic commutator feeding VSI.

Test results are recorded using a power analyzer of Fluke make and a four-channel digital storage oscilloscope of Agilent make. Test results are shown in Fig. 9(a)–(e) for various performance parameters such as starting, speed control, and PQ improvement. Smooth speed control is obtained during acceleration and deceleration by controlling the voltage at dc link as demonstrated in Fig. 9(b) and (c). Fig. 9(d) demonstrates the test results during steady-state condition at a 1500-r/min speed while the THD of current at input ac mains is recorded within 5% as shown in Fig. 9(e). These test results show conformity with the simulation results and validate the proposed voltage control scheme for speed control of PMBLDCMD along with PQ improvement at input ac mains while using a single DSP.

VII. Conclusion

A new speed control strategy for a PMBLDCMD using the reference speed as an equivalent voltage at dc link has been simulated for an air-conditioner employing a Cuk PFC converter and experimentally validated on a developed controller. The speed of PMBLDCM has been found to be proportional to the dc link voltage; thereby, a smooth speed control is observed while controlling the dc link voltage. The introduction of a rate limiter in the reference dc link voltage effectively limits the motor current within the desired value during the transient conditions. The PFC Cuk converter has ensured near unity PF in a wide range of the speed and the input ac voltage. Moreover, PQ indices of the proposed PFC drive are in conformity to the International Standard IEC 61000-3-2 [7]. The proposed PMBLDCMD has been found as a promising variable speed drive for the Air-Con system. Moreover, it may also be used in the fans with PMBLDC motor drives on the trains recently introduced in Indian Railways. These PMBLDC motor drive-based fans have similar PQ problems as they use a simple single-phase diode rectifier and no speed control. These fans also have inrush current problems. All these PQ problems of poor PF, inrush current, and speed control in these fans on the trains in Indian Railways may be mitigated by the proposed voltage-controlled PFC Cuk converter-based PMBLDCMD.

Appendix

Rated power: 0.816 kW; rated speed: 1500 r/min; rated torque: 5.2 $\mathrm{N \cdot m}$; poles: 6; stator resistance (R): 3.57 Ω/ph; inductance $(L+M)$: 9.165 mH/ph; back EMF constant (K_b): 1.3 $\mathrm{V \cdot s/rad}$; inertia (J): 0.068 $\mathrm{kg \cdot m^2}$; source impedance (Z_s): 0.03 p.u.; switching frequency of PFC switch (f_s): 40 kHz; PI speed controller gains (K_p): 0.145; (K_i): 1.85.

References

[1] T. Kenjo and S. Nagamori, *Permanent Magnet Brushless DC Motors*. Oxford, U.K.: Clarendon, 1985.

[2] T. J. Sokira and W. Jaffe, *Brushless DC Motors: Electronic Commutation and Control*. New York: Tab, 1989.

[3] J. R. Hendershort and T. J. E. Miller, *Design of Brushless Permanent-Magnet Motors*. Oxford, U.K.: Clarendon, 1994.

[4] J. F. Gieras and M. Wing, *Permanent Magnet Motor Technology—Design and Application*. New York: Marcel Dekker, 2002.

[5] B. Singh, B. N. Singh, A. Chandra, K. Al-Haddad, A. Pandey, and D. P. Kothari, "A review of single-phase improved power quality ac–dc converters," *IEEE Trans. Ind. Electron.*, vol. 50, no. 5, pp. 962–981, Oct. 2003.

[6] N. Mohan, M. Undeland, and W. P. Robbins, *Power Electronics: Converters, Applications and Design*. Hoboken, NJ: Wiley, 1995.

[7] *Limits for Harmonic Current Emissions (Equipment Input Current $\leq$ 16 A Per Phase)*, Int. Std. IEC 61000-3-2, 2000.

[8] S. Cuk and R. D. Middlebrook, "Advances in switched-mode power conversion Part-I," *IEEE Trans. Ind. Electron.*, vol. IE-30, no. 1, pp. 10–19, Feb. 1983.

[9] C. J. Tseng and C. L. Chen, "A novel ZVT PWM Cuk power factor corrector," *IEEE Trans. Ind. Electron.*, vol. 46, no. 4, pp. 780–787, Aug. 1999.

[10] B. Singh and G. D. Chaturvedi, "Analysis, design and development of single switch Cuk ac–dc converter for low power battery charging application," in *Proc. IEEE PEDES*, 2006, pp. 1–6.

[11] C. L. Puttaswamy, B. Singh, and B. P. Singh, "Investigations on dynamic behavior of permanent magnet brushless dc motor drive," *Elect. Power Compon. Syst.*, vol. 23, no. 6, pp. 689–701, Nov. 1995.

Sanjeev Singh (S'09–M'11) was born in Deoria, India, in 1972. He received the B.E. (electrical) degree from Avadhesh Pratap Singh University, Rewa, India, in 1993, the M.Tech. degree from Devi Ahilya Vishwa Vidyalaya, Indore, India, in 1997, and the Ph.D. degree from the Indian Institute of Technology Delhi, New Delhi, India, in 2011.

He joined the North India Technical Consultancy Organisation, Chandigarh, India, as a Project Officer, in 1997, and in 2000, he joined Sant Longowal Institute of Engineering and Technology, Longowal, India, as a Lecturer in the Department of Electrical and Instrumentation Engineering. He is currently an Assistant Professor in the Department of Electrical and Instrumentation Engineering, Sant Longowal Institute of Engineering and Technology. His areas of interest include power electronics, electrical machines and drives, energy efficiency, and power quality.

Dr. Singh is a Life Member of the Indian Society for Technical Education, the Systems Society of India, and The Institution of Engineers (India).

Bhim Singh (SM'99–F'10) was born in Rahamapur, India, in 1956. He received the B.E. (electrical) degree from the University of Roorkee, Roorkee, India, in 1977, and the M.Tech. and Ph.D. degrees from the Indian Institute of Technology (IIT) Delhi, New Delhi, India, in 1979 and 1983, respectively.

In 1983, he joined the Department of Electrical Engineering, University of Roorkee, as a Lecturer, and in 1988, he became a Reader. In December 1990, he joined the Department of Electrical Engineering, IIT Delhi, as an Assistant Professor, where he became an Associate Professor in 1994 and a Professor in 1997. Since September 2007, he has been the Asea Brown Boveri Chair Professor at IIT Delhi. His fields of interest include power electronics, electrical machines, electric drives, renewable energy generation, power quality, flexible ac transmission systems, and high-voltage direct-current transmission systems. He has guided 35 Ph.D. dissertations, 120 M.E./M.Tech./M.S.(R) theses, and 60 B.E./B.Tech. projects.

Dr. Singh was the recipient of the Khosla Research Prize of the University of Roorkee in 1991. He is a recipient of the J.C. Bose and Bimal K. Bose Awards of The Institution of Electronics and Telecommunication Engineers (IETE) for his contributions in the field of power electronics. He is also a recipient of the Maharashtra State National Award of the Indian Society for Technical Education (ISTE) in recognition of his outstanding research work in the area of power quality. He was the recipient of the IEEE Power and Energy Society Delhi Chapter Outstanding Engineer Award for the year 2006. He was the General Chair of the IEEE International Conference on Power Electronics, Drives and Energy Systems (PEDES'2006) held in New Delhi. He is a Fellow of the Indian National Academy of Engineering, The National Academy of Science, India, The Institution of Engineers (India), and IETE, and a Life Member of the ISTE, Systems Society of India, and National Institution for Quality and Reliability.